International Conference on Civil Engineering
Architecture & Urban Sustainable Development
27&28 November 2013, Tabriz , Iran

Application of Artificial Neural Networks to the Prediction of TBM Penetration Rate in TBM-driven Golab Water Transfer Tunnel

Yasser Mobarra[1]*, Alireza Hajian[2], Mohammadali Rahgozar[3]

1. M.Sc. Student of Geotechnical Engineering, Najafabad Branch, Islamic Azad University, Isfahan, Iran, yasermobarra@yahoo.com
2. Assistant Professor, Faculty of Nuclear Engineering and Fundamental Science, Najafabad Branch, Islamic Azad University, Isfahan, Iran, a.hajian@iaun.ac.ir
3. Assistant Professor, Faculty of Transportation Engineering, University of Isfahan, Isfahan, Iran, mohammadali-rahgozar@yahoo.com

Abstract

Rate of penetration of a Tunnel Boring Machine (TBM) in a rock environment is generally a key parameter for the successful accomplishment of a tunneling project. This paper presents the results of a study into the application of an Artificial Neural Network (ANN) technique for modeling the penetration rate of tunnel boring machines. A database, including actual, measured TBM penetration rates, uniaxial compressive strengths of the rock, the point load strength index in the rock mass and, RPM and normal force designation was established. Data collected from Golab water conveyance tunnle. A four-layer ANN was found to be optimum, with an architecture of four neurons in the input layer, 13, 4 neurons in the first, second hidden layers, respectively, and one neuron in the output layer. The correlation coefficient determined for penetration rate predicted by the ANN was 0.91.

Key words: Neural Networks, TBM, Penetration Rate, Tunnel, Rock Mass Characteristics.

1. Introduction

The penetration rate is defined as the distance excavated divided by the operating time during a continuous excavation phase. Reliable estimation of penetration rates is needed for time planning, cost control and choosing the excavation method. Making tunnel boring economic in comparison with classical drill and blasting methods requires accurate cost controls [1].

The complexity of the interaction between rock mass and the Tunnel Boring Machine (TBM) makes predicting the performance of the machine very difficult. The relationship between penetrability and rock parameters has been investigated by some re searchers [2,13].

Others have correlated TBM performance to rock mass classification systems [14,20].

Reviewing the studies mentioned above makes it clear that there is neither a unique solution nor method for modeling TBM performance in real-world projects. Methods utilizing artificial intelligence have recently been investigated by some researchers [9,21,22].

This attempts to move away from analytical solutions of mathematical formulae. Artificial Neural Networks (ANNs) have emerged as a new tool for analyzing geotechnical problems. This technique allows generalizing from a training pattern, presented initially, to the solution of the problem. Once the network has been trained with a sufficient number of sample data sets a new input having a relatively similar pattern will be predicted on the basis of the previous learning [23].

This paper presents the application of an ANN modeling technique to predicting tunnel boring machine penetration rates. For this purpose, a data set from first TBM projects was used. The main factors (rock mass and machine properties) used to predict the penetration rate in this model included the uniaxial compressive strength, the point load strength, rpm and normal force designation. The adjusted network is a good tool for predicting penetration rates during the construction of new tunnels bored in similar conditions.

2. Artificial Neural Networks

Artificial Neural Networks are simplified mathematical models inspired by the biological structure and functioning of the brain. ANN models consist of elementary processing units called neurons. The neurons are interconnected in a predefined topology called layers.

Usually the neurons operate in parallel layers [24]. A typical network topology consists of the input layer, one or more hidden layers and the output layer as shown in Figure 1.

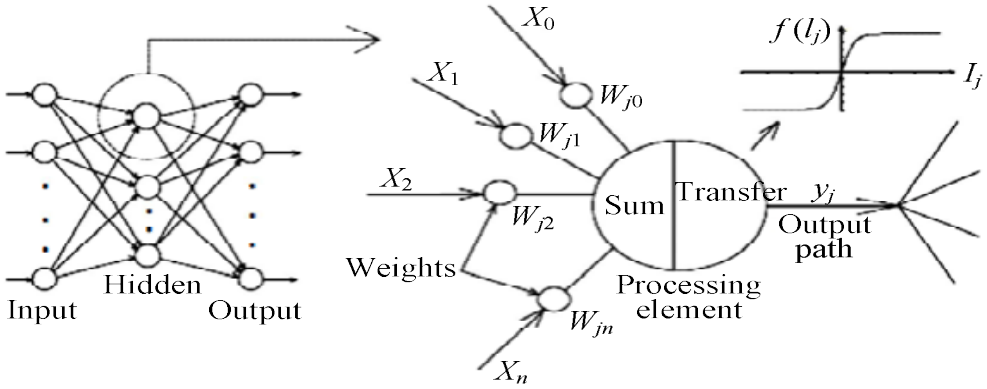

Figure 1: Typical one-hidden-layer ANN

The input from each Processing Element (PE) in the previous layer (X_i) is multiplied by an adjustable connection weight, w_{ij}. the weighted input signal are summed at each PE and a threshold value (θ_j) is added. This combined input (I_j) is then passed through a non-linear transfer function, *f*, to produce the output of the PE y_j . The output of one PE pro vides the input to the PE's in the next layer. This process is summarized in Equations (1) and (2) and illustrated in Figure 1 [25].

$$I_j = \sum_{j=1}^{n} w_{ji} + \Theta_j \quad \text{, summation} \qquad (1)$$

$$Y_j = f(I_J) \quad , \quad \text{Transfer} \tag{2}$$

The transfer functions are designed to map a neuron, or layer, net output to its actual output. They are simple linear or nonlinear step functions. The type of these transfer functions depends on the purpose of the neural network. Nonlinear (LOGSIG, TANSIG) and linear (POSLIN, PURELIN) functions can be used as transfer functions, see Figure 2. The most familiar and effective function in our case is the Logarithmic Sigmoid function (LOGSIG) defined as [26]:

$$F=1/1+\exp(-av) \tag{3}$$

where v is the weighted sum of the inputs for a processing unit and a is a constant that typically varies between 0 and 1.00.

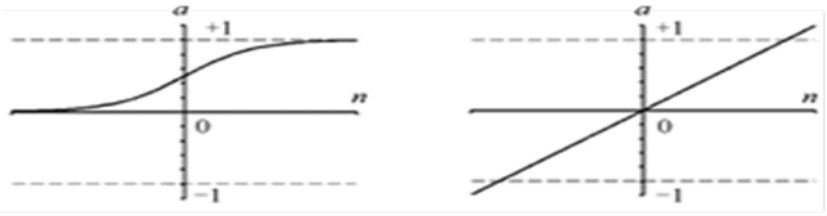

(a) Sigmoid (b) Liner

Figure 2: Typical sigmoid and liner transfer function [26]

The neural network is first trained by processing a large number of data sets. After completion of proper training neural networks can detect similarities when presented with a new pattern. This results in a predicted output pattern. Any particular network can be defined using three fundamental components; a transfer function, a network architecture and a learning law [27].

3. Training of the Network

During the training phase data consisting of input and associated output pairs that represent the problem at hand are processes with the network. Various algorithms are available for training of neural networks but the back-propagation algorithm is the most versatile and robust technique. It provides the most efficient learning procedure for multilayer perception neural networks [28].
Multiple layers of neurons with nonlinear transfer functions allow the network to learn nonlinear and linear relationships between given input and output vectors. A forward pass is made during training when data is processed through the input layer to the hidden layer and thence to the output layer. During the backward pass the network's actual output (from the previous forward pass) is compared to the target output. Error estimates are computed from the comparison. The weight associated with an output unit can be adjusted to reduce the error. This process is repeated for all training pairs in the data set until the network error converges to a threshold (minimum error) defined by some corresponding cost function [26].

Dates its weights incrementally after seeing each input-output pair. After it has seen all the input-output pairs and adjusted its weights many times it is said that one epoch has been completed. The process is then repeated for as many epochs as needed until an error within the user specified goal is reached [9].

4. Input Parameters

It is difficult to determine all the relevant parameters that influence the prediction of penetration rate. However, not all the parameters are independent and some of them are strongly correlated. Hence, it was not important to use all the variables as input parameters. The selected parameters affecting Rate of Penetration (ROP) used in this study were: Uniaxial Compressive Strength of the rock (UCS), point load strength index ($I_{S(50)}$), RPM and normal force (f_n). Each parameter has an important effect on TBM performance. Although machine characteristics (e.g., thrust or torque) are very important for overall performance it was assumed here that these characteristics remain unchanged. In-other-words, all possible effects were directly caused by the geotechnical and machine conditions.
Data were obtained from Golab water conveyance tunnel projects:
The main purpose of Golab tunnel project was the transfer of water from Tanzimi dam river to Kashan, along with supplying Karoun desert with water from the Zayande-Rud. The area of the project is located in the west of Isfahan with in the distance of 100 kilometers and the north of Chaharmahal-o-Bakhtiari Province, and the nearest towns to this project are Tiran and Chadegan. The highest mountain range of this region is the Dadan mountain range with the height of 3890 meters and the lowest point of this region belongs to the Zayande-Rud valley with the height of 1900 meters [30].

5. The Geotechnical Studies of the Tunnel Route

Due to the request of the project supervisor, nine geotechnical boreholes were dug to the total length of 3105 meters in the ten kilometer route of the Golab tunnel as well as two other boreholes in the location of the water entrance to the length of 100 meters totally by Azemooneh Foolad Company. The drillings were carried out with rotary and continuous core drilling, then borehole and laboratory tests were done by the foregoing company. The purpose followed in this drillings was to obtain more geotechnical information from the depth of the tunnel in boreholes [31].

6. Rock Mass Characteristics in Golab Tunnel

The digging of this tunnel lasted as long as 290 days. During the drilling, the drilling machine faced some problems in different units of rock bed leading to stopping drilling. The rock units containing Quartz Muscovite, Granite Gneiss, Actinolite Schist, Meta-Sandstone and Biotite Schist were the main drilled units in most of the tunnel drilling period. A part of the tunnel is shown in Figure 3. In some month of drilling, the tunnel ran into other rock units such as Phyllite, Monzodiorite, Slate and Conglomerate rocks. As the names of these rock units indicate, some have low strength or average strength. Table 1 represents the summary of Golab water transfer tunnel and the parameters of TBM [32].

Table 1: Summary of Golab Tunnel and Parameters of TBM

Tunnel diameter	4.525 m
Tunnel length	10 km
Machine type	TB453E/TS
Maximum torque	557 kN.m
Maximum thrust force	8900 kN
Cutters diameter	17 in
Number of cutters	36
Maximum revolution per minute	12 rpm

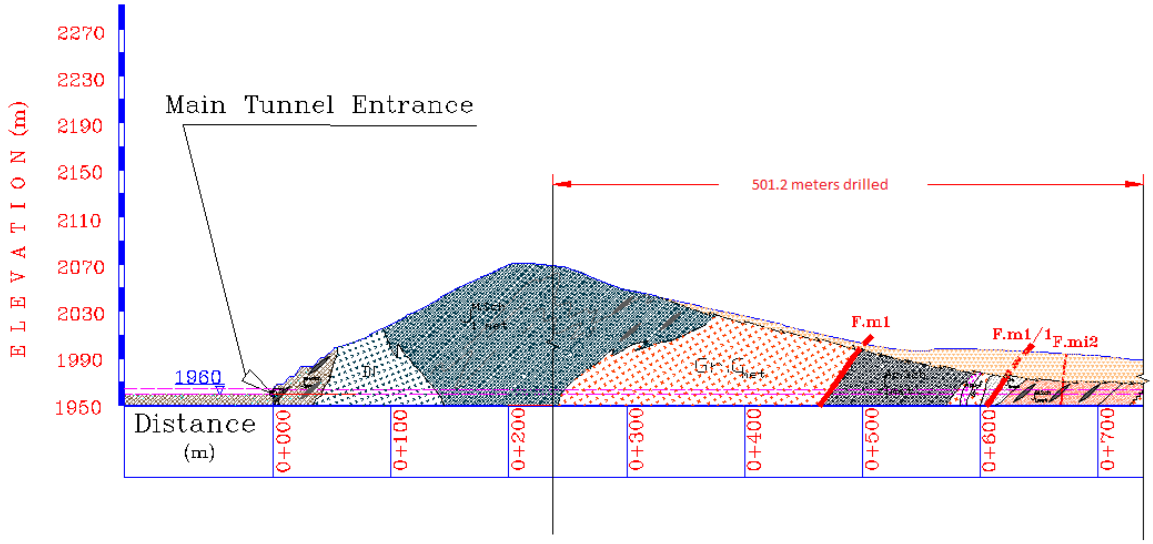

Figure 3: A Part of the Golab Tunnel

7. Input Dataset

One of the most important stages in the ANN technique is data collection. Before training and implementation, the data set was divided randomly into training, validation and test subsets.

In the present study, 289 data sets were collected. From these, 65% of the data were chosen for training, 15% for validation and 20% for the final test. These data are given in Table 2.

The training set was used to generate the model and the validation set was used to check the generalization capability of the model.

Table 2: Rock and Machine Properties and the Measured ROP for Golab Tunnel

NO	F_n (KN)	RPM	$I_{S(50)}$ (MPa)	6_C (MPa)	ROP (Cm/hr)	NO	F_n (KN)	RPM	$I_{S(50)}$ (MPa)	6_C (MPa)	ROP (Cm/hr)
1	112.5	7.6	2.25	31	475.08	34	108.3333	5.2	2.25	31	437.26
2	125	8.6	4.3268	37	449.49	35	109.7222	4.9	2.25	31	424.81

3	138.8889	9	4.3268	37	533.88	36	120.8333	6	2.25	31	381.5
4	129.1667	10.7	4.3268	37	524.45	37	140.2778	10.5	2.25	31	477.98
5	136.1111	10	4.3268	37	441.25	38	127.7778	9.5	4.7520	45	461.06
6	127.7778	10.1	4.3268	37	408.11	39	118.0556	5.5	3.9424	31	260.96
7	93.0556	8.7	4.3268	37	501.45	40	137.5	8	3.6822	27.5	366.33
8	129.1667	9.7	4.3268	37	441.32	41	133.3333	6	3.6822	27.5	436.19
9	141.6667	11.5	4.3268	37	307.07	42	123.6111	6.25	3.6822	27.5	447.85
10	111.1111	9.1	4.3268	37	421.32	43	118.0556	6	2.25	25	497.65
11	104.1667	6.4	4.3268	37	467.93	44	120.8333	8.6	2.25	25	410.18
12	111.1111	9.6	2.25	25	430.82	45	136.1111	7.1	2.25	25	471.76
13	111.1111	7.9	2.25	25	512.65	46	129.1667	6.7	2.25	25	516.99
14	105.5556	6.1	2.25	25	488.66	47	148.6111	9.5	2.25	31	480.33
15	91.6666	5.9	2.25	25	405.61	48	134.7222	7.7	2.25	31	455.3
16	100	3.3	2.25	25	443.5	49	130.5556	8	2.25	31	461.18
17	126.3889	9.1	3.2463	22.5	612.86	50	130.5556	7.2	2.25	31	468.85
18	108.3333	3.2	2.25	26	309.35	51	129.1667	5.5	2.25	31	535.11
19	109.7227	4.1	2.25	26	276.62	52	133.3333	6.5	2.25	31	540.67
20	108.3333	5.6	2.25	26	489.74	53	129.1667	7.1	2.25	31	501.78
21	109.7227	6.5	2.25	26	620.42	54	145.8333	10.2	2.25	31	535.45
22	119.4444	7.8	2.25	26	520.66	55	126.3889	8.2	2.25	31	526.53
23	90.2778	6.7	4.3268	37	323.23	56	125	9	2.25	31	512.53
24	100	6.2	4.3268	37	492.57	57	129.1667	8.3	2.25	31	512.62
25	100	5.9	4.3268	37	547.36	58	125	6.5	2.25	31	402.89
26	104.1667	6.45	4.3268	37	494.45	59	109.7222	5.5	2.25	31	384.28
27	100	6.6	4.3268	37	422.2	60	130.5556	7.7	2.25	31	467.04
28	84.7222	6.6	4.3268	37	264.8	61	115.2778	7	2.25	31	492.4
29	87.5	3.75	2.25	31	420.16	62	127.7778	8.8	2.25	31	383.87
30	54.1667	1.7	2.25	31	396.46	63	119.4444	7.7	2.25	31	394.61
31	98.6111	5.65	2.25	31	408.79	64	141.6667	9.4	2.25	31	451.93
32	88.8888	5	2.25	31	427.15	65	147.2222	9.9	2.25	24	429
33	108.3333	4.9	2.25	31	433.95	66	108.3333	9	2.25	24	471.04
67	129.1667	8.3	2.25	24	426.07	102	129.1667	4.3	2.25	24	568.53
68	133.3333	7.5	2.25	31	456.09	103	126.3889	4.4	2.25	24	529.46

69	126.3889	8.85	2.25	31	504.78	104	123.6111	4.9	2.25	24	544.84
70	118.0556	7.7	2.25	31	390.57	105	108.3333	4.9	3.3865	24	501.9
71	120.8333	7	2.25	31	411.37	106	112.5	4.6	2.4	27.5	536.54
72	123.6111	7.4	2.25	31	472.11	107	109.7222	4.5	2.25	24	543.71
73	134.7222	8.9	2.25	31	446.86	108	125	4.9	2.25	24	633.65
74	123.6111	7	2.25	31	532.69	109	113.8889	3.9	2.25	24	544.99
75	127.7778	6.4	2.25	32	470.82	110	136.1111	4.6	4.5	95	300.77
76	115.2778	3.8	2.25	32	322.44	111	140.2778	4.6	2.25	31	527.8
77	104.1667	3.8	2.25	32	335.11	112	123.6111	4.4	2.4	31	544.69
78	126.3889	6.3	2.25	31	494.19	113	120.8333	4.5	2.25	31	550.23
79	113.8889	6.4	2.25	31	499.6	114	123.6111	4.3	2.4	27.5	577.46
80	125	6.3	2.25	31	452.62	115	122.2222	4.3	2.25	31	520.73
81	102.7778	6	2.25	31	591.74	116	129.1667	4.2	2.25	31	616.22
82	126.3889	6.4	2.25	31	515.02	117	113.8889	4.2	2.25	31	652.42
83	137.5	7.8	2.25	31	402.21	118	122.2222	4.4	2.25	31	557.8
84	122.2222	6.2	2.25	31	466.28	119	138.8889	4.8	2.25	31	534.44
85	118.0556	7.1	2.25	31	584.87	120	119.4444	5	6.4	95	498.86
86	137.5	6	2.25	31	526.02	121	131.9444	4.7	2.25	31	571.19
87	112.5	5.3	2.25	31	496.29	122	134.7222	4.5	2.25	31	602.28
88	130.5556	5.5	2.25	31	536.44	123	134.7222	4.7	2.25	31	622.37
89	116.6667	7.3	2.25	31	330.83	124	151.3889	5.8	2.25	31	540.57
90	37.5	1	2.25	31	140	125	123.6111	5.6	2.25	31	628.99
91	127.7778	1.7	6.4	83	362.75	126	126.3889	5.6	2.25	31	591.48
92	115.2778	4.8	2.25	24	510.08	127	130.5556	6	2.25	31	597.47
93	125	4.1	2.25	24	517.95	128	147.2222	5.6	2.25	31	487.01
94	131.9444	5.2	2.25	24	516.37	129	163.8889	5.9	6.4	95	447.92
95	137.5	4.5	2.25	24	490.74	130	134.7222	6	2.25	31	485.59
96	119.4444	5.7	2.25	24	481.47	131	125	5.4	2.25	31	500.63
97	122.2222	4.9	2.25	24	583.98	132	127.7778	5.4	2.25	31	482.26
98	120.8333	5.7	2.4	26	537.16	133	119.4444	5.2	2.25	31	412.57
99	113.8889	4.5	2.25	26	511.44	134	118.0556	3.8	2.25	31	452.14
100	123.6111	5	2.25	24	488.06	135	129.1667	4.8	2.25	31	521.55
101	115.2778	5.7	2.25	24	519.62	136	126.3889	4.6	2.25	31	488.95
137	126.3889	5	2.25	31	542.57	173	166.6667	4.1	1.075	20	642.99
138	129.1667	4.3	2.25	31	569.85	174	151.3889	4.5	1.075	83	729.73

139	125	4.4	2.25	31	590.82	175	138.8889	3.95	1.075	20	727.84
140	129.1667	4.7	2.25	31	591.45	176	144.4444	3.76	1.075	20	800.79
141	143.0556	5	2.25	31	477.86	177	134.7222	4.06	1.075	20	568.89
142	122.2222	4.3	2.25	31	555.03	178	137.5	3.36	1.075	20	554.31
143	113.8889	3.7	2.25	31	573.74	179	137.5	3.7	1.075	20	572.99
144	115.2778	3.9	2.25	31	600.9	180	150	3.7	1.075	20	500.2
145	127.7778	5	2.25	31	428.89	181	130.5556	4	1.075	20	439.19
146	101.3889	5.2	2.25	31	82.53	182	123.6111	4.1	1.075	20	588.21
147	113.8889	4.1	2.25	31	513.72	183	148.6111	4.9	1.075	20	566.12
148	130.5556	4.2	2.25	31	475.92	184	134.7222	4.4	1.075	20	640.81
149	133.3333	4.4	2.25	31	677.34	185	140.2778	4.6	1.075	20	653.96
150	131.9444	4.8	2.25	31	633.12	186	129.1667	4.1	1.075	20	670.18
151	130.5556	4.4	2.25	31	642.3	187	131.9444	4.6	1.075	20	659.17
152	150	5	2.25	31	602.44	188	115.2778	4.5	1.075	20	610.5
153	140.2778	4.2	2.25	4.5	538.27	189	127.7778	4.5	1.075	20	663.27
154	125	4.8	4.5	4.5	533.7	190	123.6111	4.3	1.075	20	652.52
155	138.8889	5.3	2.25	24	491	191	106.9444	4.1	1.075	20	662.39
156	156.9444	6.2	2.25	24	586.46	192	113.8889	3.5	1.075	83	619.05
157	119.4444	6.4	2.25	24	639.23	193	150	5.2	1.075	83	595.68
158	136.1111	5.2	4.5	83	556.92	194	127.7778	6.5	6.4	83	752.86
159	138.8889	4.3	4.5	83	576	195	106.9444	4.1	6.4	83	20.97
160	115.2778	3.7	1.075	20	585.15	196	88.8888	3.8	6.4	83	508.39
161	147.2222	2.9	1.075	20	491.09	197	84.7222	3.8	6.4	83	431
162	129.1667	3.3	1.075	20	581.64	198	91.6666	3.6	1.075	83	448.67
163	147.2222	7.5	4.5	83	483.07	199	66.6666	4.1	6.4	83	395.38
164	143.0556	7.1	4.5	83	520.35	200	145.8333	5.3	6.4	83	372.57
165	104.1667	3.5	4.5	83	557.52	201	125	5.5	1.075	20	401.46
166	133.3333	3.6	4.5	83	595.81	202	95.8333	3.3	1.075	20	381.66
167	116.6667	3.9	1.075	9.5	503.58	203	87.5	3.3	1.075	20	500.8
168	166.6667	4.4	4.5	83	603.69	204	109.7222	3.7	1.075	20	500.97
169	141.6667	5.4	6.4	83	585.4	205	127.7778	3.95	6.4	83	383.11
170	151.3889	7.3	1.075	20	565.65	206	106.9444	7.6	1.075	20	413.49
171	150	8.1	1.075	20	524.6	207	91.6667	4	1.075	20	491.9
172	151.3889	5.4	1.075	20	729.26	208	87.5	3.6	1.075	20	469
209	98.6111	3.6	1.075	20	533.68	245	93.0555	3.9	1.075	20	588.93
210	108.3333	6.2	6.4	83	472.48	246	97.2222	3.9	1.075	20	558.53

211	136.1111	5.8	6.4	83	413.97	247	94.4444	4.03	1.075	20	624.05
212	150	7.2	6.4	83	586.53	248	84.7222	3.53	0.15	6	528.45
213	125	4.8	6.4	83	488.52	249	79.1667	3.5	0.15	6	637.06
214	120.8333	6	6.4	83	561.86	250	77.7777	3.16	0.15	6	551.75
215	98.6111	4.3	1.075	20	704.86	251	91.6666	3	0.15	6	538.45
216	108.3333	3.8	1.075	20	502.44	252	79.1666	3.1	0.15	6	601.61
217	97.2222	4	1.075	20	442.74	253	80.5555	3.2	0.15	6	536.46
218	109.7222	3.6	6.4	83	564.09	254	75	2.8	0.15	6	487.89
219	108.3333	3.7	6.4	83	577.08	255	77.7777	2.5	0.15	6	539.76
220	115.2778	4.2	6.4	83	518.6	256	95.8333	3.6	0.15	6	549.95
221	100	3.9	1.075	20	568	257	101.3889	3.2	0.15	6	519.03
222	137.5	5.4	6.4	83	571.44	258	106.9444	3.2	0.15	6	456.66
223	115.2778	4.2	6.4	83	572.52	259	87.5	2.7	0.15	6	322.18
224	154.1667	5	6.4	83	543	260	97.2222	2.8	0.15	6	473.38
225	95.8333	3.1	1.075	20	543.6	261	118.0556	4.7	0.15	6	500.18
226	180.5556	11	6.4	83	474.29	262	126.3889	5.9	6.4	83	481.94
227	152.7778	10.3	6.4	83	208.38	263	94.4444	4.8	0.15	6	470.47
228	102.7778	8.4	6.4	83	431.25	264	87.5	3.2	0.15	6	552.41
229	80.5555	6.7	6.4	83	462.15	265	97.2222	3.2	0.15	6	496.26
230	115.2778	8.3	6.4	83	344.21	266	106.9444	3.7	0.15	6	537.85
231	131.9444	10.8	6.4	83	311.05	267	122.2222	5.6	0.15	6	563.36
232	81.9444	4	6.4	83	598.53	268	104.1667	3.5	0.15	6	594.03
233	86.1111	4	1.075	20	503.48	269	120.8333	3.7	0.15	6	521.7
234	87.5	2.5	1.075	20	433.92	270	127.7778	4.4	0.15	6	551.33
235	136.1111	7.5	3.25	90	332.22	271	104.1667	3.1	0.45	4.25	611.04
236	136.1111	12	3.25	90	104.67	272	108.3333	3.96	0.45	4.25	561.08
237	186.1111	11	3.25	90	192.61	273	172.2222	4.9	0.45	4.25	581.79
238	127.7778	7.6	1.075	20	547.21	274	172.2222	5	0.45	4.25	155.68
239	130.5556	6.3	1.075	20	460.9	275	138.8889	6.2	0.45	4.25	490.7
240	94.4444	6.4	1.075	20	671.1	276	86.1111	2.9	0.45	4.25	720.18
241	101.3889	5.3	1.075	20	486.51	277	86.1111	2.4	0.45	4.25	552.46
242	156.25	9.8	1.075	20	410.3	278	111.1111	2.7	0.45	4.25	522.66
243	109.7222	6.8	6.4	83	546.38	279	168.0556	2.83	0.45	4.25	375.26
244	101.3889	3.9	1.075	20	573.73	280	133.3333	2.76	0.45	4.25	447.73

281	131.9444	3.73	0.45	4.25	562.6	286	138.8889	3.8	0.45	4.25	621.79
282	138.8889	5.66	0.45	4.25	621.73	287	133.3333	4.06	0.45	4.25	583.84
283	133.3333	3.73	0.45	4.25	679.45	288	147.2222	3.83	0.45	4.25	657.84
284	172.2222	3.4	0.45	4.25	683.09	289	134.7222	4.7	0.45	4.25	658.98
285	130.5556	3.36	0.45	4.25	665.33	290	-	-	-	-	-

8. ANN Topology

An appropriate architecture was obtained from feed-forward back propagation. A three-layer network with logarithmic sigmoid transfer function neurons in the hidden layer, and a purely linear transfer function neuron corresponding to ROP in the output layer, was chosen. Since there is no direct, precise way of determining the most appropriate number of hidden layers, and number of neurons in each hidden layer, a trial and error procedure is typically used to identify the best network for a particular problem. Several network topologies were examined for this work. The Levenberg-Marquardt algorithm was chosen for training the ANNs because it is known to be the fastest method for training moderate-sized feed-forward neural networks. The resulting target network should produce a minimum error for the training pattern and give a generalized solution that performs well with the testing pattern.

9. Testing and Validation of the ANN Model

Testing and validation of the ANN model was done with new data sets. These data were not previously used while training the network. The results are presented in this section to demonstrate the performance of the networks. The Mean Squared Error (MSE) and coefficient of correlation between the predicted and measured values were taken as the performance measures. The MSE was calculated as:

$$MSE = 1/Q \sum_Q (d-o)^2 \quad (4)$$

where d, o and Q represent the predicted output, the measured output and the number of input-output data pairs, respectively. The prediction was based on the input data sets shown above. The quality of the results obtained for some of the models is shown in Table 3. The correlation coefficients and mean squared errors for the different models are presented there.

Table 3: Comparison Between Some of the Models

R	MODEL		MSE(Train)	MSE(validation)	MSE(Test)	R(Test)	R(All)
1-	4-4-1	s-p	$5e^{-5}$	$1.22e^{-5}$	$4.98e^{-3}$	0.111	0.955
2-	4-7-1	s-p	$9.81e^{-17}$	$4.615e^{-5}$	0.1	0.131	0.705
3-	4-8-1	s-p	$10e^{-4}$	0.0118	$10e^{-4}$	0.147	0.637
4-	4-10-1	S-p	$6.7e^{-4}$	0.0146	$9.5e^{-4}$	0.513	0.630
5-	4-15-1	s-p	$7.9e^{-11}$	0.00971	0.00971	0.289	0.68
6-	4-12-10-1	s-s-p	$10e^{-15}$	0.00197	0.00197	0.84	0.905
7-	4-7-4-1	s-s-p	$1.894e^{-5}$	$1.894e^{-5}$	0.00165	0.227	0.954

8-	4-13-4-1	s-s-p	$8.451e^{-6}$	0.00338	$1.116e^{-6}$	0.923	0.913
9-	4-14-4-1	s-s-p	$1.188e^{-19}$	0.00557	0.00557	0.402	0.723
10-	4-15-4-1	s-s-p	0.00770	0.00973	0.00475	0.38	0.45
11-	4-8-5-1	s-s-p	0.00017	0.01241	0.00020	0.316	0.530
12-	4-13-5-1	s-s-p	0.00046	0.00141	$2.37e^{-5}$	0.297	0.938
13-	4-7-7-1	s-s-p	$6.34e^{-21}$	0.00294	$1.71e^{-5}$	0.301	0.911
14-	4-15-10-1	s-s-p	0.00044	0.01913	0.00083	0.428	0.313
15-	4-17-1	s-p	$9.6e^{-4}$	0.00002	0.00034	0.465	0.809
16-	4-6-5-1	s-s-p	0.000197	0.000345	0.000345	0.86	0.90
17-	4-12-9-5-1	s-s-s-p	$2.95e^{-9}$	$2.12e^{-5}$	0.00221	0.69	0.94
18-	4-12-9	s-s-p	$1.78e^{-13}$	$2.37e^{-5}$	0.00222	0.36	0.94
19-	4-4-7-2-1	s-s-s-p	$7.12e^{-11}$	$2.11e^{-5}$	0.02483	-0.08	0.009
20-	4-9-3-1	s-s-p	$6.92e^{-6}$	$1.57e^{-5}$	0.00204	0.65	0.94

The errors suggest the network with a 4-13-4-1 architecture is the optimum one. This network is shown in Figure 4.

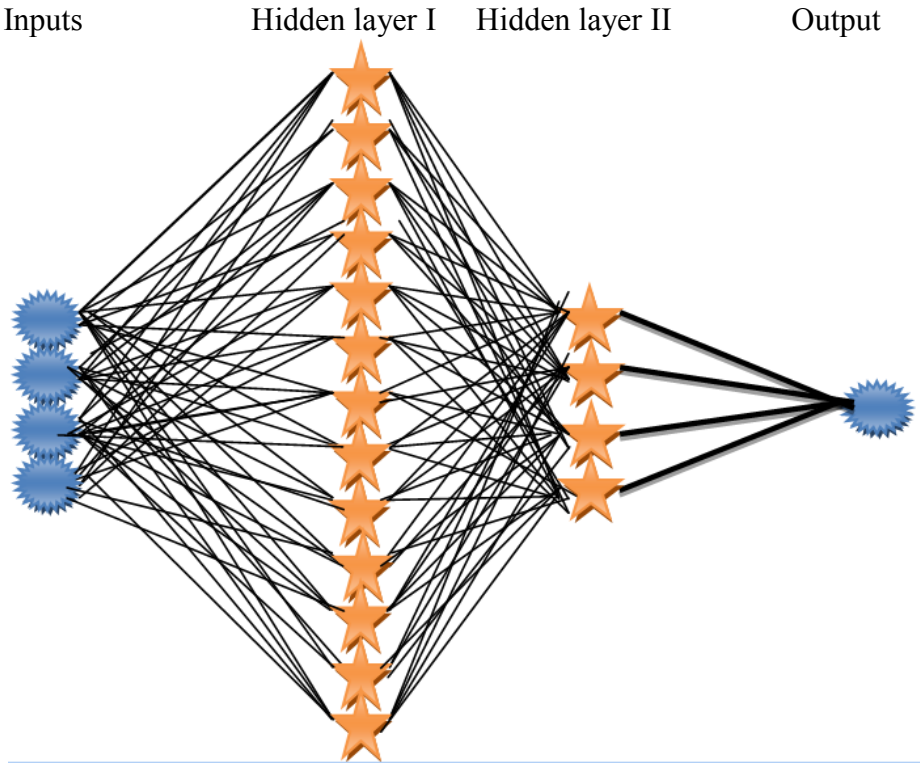

Figure 4: Suggested ANN for Predicting ROP

10. Results and Discussion

Figure 5 shows a graph comparing the measured and predicted data for the preferred ANN model. It appears that the ROP model has predicted values close to the measured ones: the correlation coefficient between measured and predicted ROP is very high.

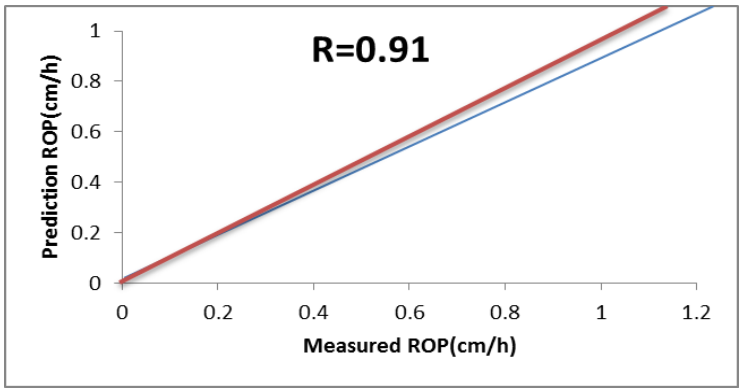

Figure 5: Correlation Between the Measured and Predicted Values of ROP

11. Conclusion

The results obtained from this research show that an ANN is a useful means to predict penetration rate of a TBM. However, the relationship among the inputs and outputs is very complex. The results obtained are still highly encouraging and satisfactory. The optimum ANN architecture was found to be four neurons in the input layer, two hidden layers with 13 and 4 neurons and one neuron in the output layer. Since a neural network can update "its" knowledge over time if more training data sets are processed neural networks will result in a greater accuracy and more robust prediction than any other analysis technique. They prove to be economical and easier in comparison to expensive experimental work. Since the model is based on geotechnical and machine data the prediction of the penetration rate may be used to identify risk-prone areas. The high correlation coefficient and low error allow the conclusion that the data selected as input parameters are suitable and have an affect on ROP. The investigation described in this paper used data collected from Golab Tunnel. There may have been an effect on these data since different teams worked on the different faces.

References

[1] Alber M. Prediction of penetration, utilization for hard rock TBMs. *In*: *Proceedings of the International Conference of Eurock*. Rotterdam: Balkema, 1996: 721-725.

[2] Graham P C. Rock exploration for machine manufacturers. *In*: *Proceedings of Symposium on Exploration for Rock Engineering.* Rotterdam: Balkema, 1976: 173-180.

[3] Farmer I W, Glossop N H. Mechanics of disccutter penetration. *Tunnel Int*, 1980, 12(6): 22-25.

[4] Cassinelli F, Cina S, Innaurato N, Mancini R, Sampaolo A. Power consumption and metal wear in tunnel-boring machines: analysis of tunnel boring machine operation in hard rock. *Tunneling*, 1982, 82: 73-81.

[5] O'Rourke J E, Spring J E, Coudray S V. Geotechnical parameters and tunnel boring machine performance at goodwill tunnel, California. *In*: *Proceedings of the 1st North American Rock Mechanics Symposium*. Rotterdam: Balkema, 1994.

[6] Rostami J. *Development of a Force Estimation Model for Rock Fragmentation with Disc Cutters through Theoretical Modeling and Physical Measurement of Crushed Zone Pressure* [Ph.D. dissertation]. Colorado: Colorado School of Mines, 1997.

[7] Bruland A. *Hard Rock Tunnel Boring* [Ph.D. dissertation]. Trondheim: Norwegian University of Science and Technology, 1998.

[8] Cheema S. *Development of a Rock Mass Boreability Index for the Performance of Tunnel Boring Machines* [Ph.D. dissertation]. Colorado: Colorado School of Mines,1999.

[9] Grima M A, Bruines P A, Verhoef P N W. Modeling tunnel boring machine performance by neuro-fuzzy methods. *Tunn Undergr Space Technol*, 2000, 15: 259-269.

[10] Yagiz S. *Development of Rock Fracture and Brittleness Indices to Quantify the Effects of Rock Mass Features and Toughness in the CSM Model Basic Penetration for Hard Rock Tunneling Machines* [Ph.D. dissertation]. Colorado: Department of Mining and Earth Systems Engineering, 2002.

[11] Yagiz S. Utilizing rock mass properties for predicting TBM performance in hard rock conditions. *Tunn Un dergr Space Technol*, 2008, 23(3): 326-339.

[12] Gong Q M, Zhao J. Development of a rock mass characteristics model for TBM penetration rate prediction. *Int J Rock Mech Mining Sci*, 2009, 46(1): 8-18.

[13] Mikaeil R, Zare M, Sereshki F. Multifactorial fuzzy approach to the penetrability classification of TBM in hard rock conditions. *Tunn Undergr Space Technol*, 2009, 24(3): 500-505.

[14] Blindheim O T. *Boreability Predictions for Tunneling* [Ph.D. dissertation]. Trondheim: Norwegian Institute of Technology, 1979.

[15] Bamford W F. Rock test indices are being successfully correlated with tunnel boring machine performance. *In*: *Proceedings of the 5th Australian Tunneling Conference*. Rotterdam: Balkema, 1984: 9-22.

[16] Innaurato N, Mancini R, Rondena E, Zaninetti A. For casting and effective TBM performance in a rapid excavation of a tunnel in Italy. *In*: *Proceedings of the 7th In- ternational Congress Rock Mechanics.* Rotterdam: Balkema, 1991: 1009-1014.

[17] Rostami J, Ozdemir L. A new model for performance prediction of hard rock TBM. *In*: *Proceedings of RETC*. Rotterdam: Balkema, 1993: 793-809.

[18] Sundaram N M, Rafek A G, Komoo I. The influence of rock mass properties in the assessment of TBM performance. *In*: *Proceedings of the 8th International IAEG Congress*. Rotterdam: Balkema, 1998: 3353-3359.

[19] Bruland A. *Hard Rock Tunnel Boring* [Ph.D. dissertation]. Trondheim: Norwegian Institute of Technology, 1998.

[20] Sapigni M, Berti M, Bethaz E, Busillo A, Cardone G. TBM performance estimation using rock mass classifications. *Int J Rock Mech Mining Sci*, 2002, 39: 771-788.

[21] Okubo S, Fukui K, Chen W. Expert system for applica bility of tunnel boring machine in Japan. *Rock Mechanics and Rock Engineering*, 2003, 36(4): 305-322.

[22] Benardos A G, Kaliampakos D C. Modeling TBM performance with artificial neural networks. *Tunn Underground Space Technol*, 2004, 19(3): 597-605.

[23] Khandelwal M, Roy M P, Singh P K. Application of artificial neural network in mining industry. *Ind Min Eng J*, 2004, 43: 19-23.

[24] Menhrotra K, Mohan C K, Ranka S. *Elements of Artificial Neural Networks.* Cambridge: MIT Press, 1997.

[25] Shahin M, Jaksa M, Maier H. Artificial neural networks application in geotechnical engineering. *Australian Geomechanics*, 2001, 36(1): 49-62.

[26] Hasanipak A. *Exploratory Data Analysis.* Tehran: University of Tehran Press, 2004. (In Persian).

[27] Simpson P K. *Artificial Neural System*: *Foundation*, *Paradigm*, *Application and Implementations*. New York: Pergamon Press, 1990.

[28] Tawadrous A S, Katsabanis P D. Prediction of surface crown pillar stability using artificial neural networks. *Int J Num Anal Methods Geomech*, 2006, 31: 917-931.

[29] Oraee K, Salehzade H, Salehi B. Calculation of effi- ciency and advanced rate TBMs in Karaj-Tehran water transfer project using practical models. *In*: *Proceedings of the 4th National Congress on Civil Engineering*. Tehran, 2008. (In Persian).

[30] E. Sharifi, "Engineering geological studies of Golab water transfer tunnel", Imensazan Consulting Engineers, 2009.

[31] A. Tourgoli, "Report of the generalities of Golab water transfer tunnel", Separsang Construction Company, 2006.

[32] A. Eftekhari, M. Tofighi, "Golab water transfer tunnel project engineering services' monthly report of the engineering geology and mechanized drilling", 2009.